PNAS NEXUS

PNAS Nexus, 2025, 4, pgaf161
https://doi.org/10.1093/pnasnexus/pgaf161
Advance access publication 21 May 2025
Research Report

Rapid diagnosis of ocular viral infections via single-virus detection using solid-state nanopore: A diagnostic evaluation study

Noriyasu Hashida[a,b,*], Hiroyasu Takei[c], Masateru Taniguchi[d], Norihiko Naono[b], Takeshi Soma[a], Yoshinori Oie[a], Kazuichi Maruyama[b,e], Lidya Handayani[f], Yasuko Mori[f], Andrew Quantock[g] and Kohji Nishida[a,b,e,*]

[a]Department of Ophthalmology, Osaka University Graduate School of Medicine, Room E7, 2-2 Yamadaoka, Suita, Osaka 565-0871, Japan
[b]Integrated Frontier Research for Medical Science Division, Institute for Open and Transdisciplinary Research Initiatives (OTRI), Osaka University Graduate School of Medicine, Osaka 565-0871, Japan
[c]Aipore Inc., Tokyo 150-8512, Japan
[d]The Institute of Scientific and Industrial Research, Osaka University, Osaka 565-0871, Japan
[e]Department of Vision Informatics, Graduate School of Medicine, Osaka University, Suita, Osaka 565-0871, Japan
[f]Division of Clinical Virology, Center for Infectious Diseases, Kobe University Graduate School of Medicine, Kobe 650-0017, Japan
[g]Structural Biophysics Group, School of Optometry and Vision Sciences, Cardiff University, Wales, Cardiff CF10 3AT, United Kingdom
*To whom correspondence should be addressed: Email: knishida@ophthal.med.osaka-u.ac.jp (K.N.); Email: nhashida@ophthal.med.osaka-u.ac.jp (N.H.)
Edited By Youfang Cao

Abstract

Rapid and precise identification and discrimination of causative pathogens are required in the treatment of infectious diseases. Quantitative real-time PCR is used to detect and identify infectious viruses before treatment. Although it is an established modality, results take several hours, even in well-equipped hospitals. It is difficult to simultaneously detect many pathogen types because only a single-virus genome can be amplified per PCR. Recently, an AI-based nanopore machine has been used to identify individual viruses based on electrical conductivity. Here, we recognized a single virus using an AI-based detection system and successfully identified viral particles in clinical samples without the need for any prior treatment. We used a nanopore detector and discriminated among viruses using an AI-based waveform analysis. The efficacy of the AI nanopore detector as an on-site clinical analysis device was validated in cultured herpesvirus samples, and its discrimination capability was verified with clinical samples. The AI nanopore analysis of cultured viruses revealed that *Alphaherpesvirinae* and *Betaherpesvirinae* within the same *Herpesviridae* family can be distinguished with a relatively high accuracy. The AI nanopore rapidly detected viral particles and can be useful as an on-site clinical diagnosis tool. We demonstrated the multiplex discrimination of herpetic viruses in clinical ocular samples, proving that the AI nanopore is an ultra-high-speed and highly sensitive detection tool that can be used in various medical fields.

Keywords: virus, infection, ocular, single-virus detection, solid-state nanopore

Significance Statement

Infectious diseases, notably viral infections, present formidable clinical challenges due to rapid progression, demanding early and precise pathogen detection for effective intervention. Conventional PCR techniques, although prevalent, are limited by time constraints and lack the ability to discern viral viability. This study introduces a pioneering AI-enhanced nanopore technology capable of detecting individual herpesvirus particles with exquisite sensitivity and specificity by analyzing real-time current waveforms. This approach not only identifies live viruses with exceptional accuracy but also demonstrates versatility in identifying a range of pathogens, including novel viral entities, through waveform pattern recognition. This AI-nanopore platform represents a transformative, expedient, and economically viable alternative to traditional PCR, poised for integration into clinical diagnostics, thus advancing the landscape of infectious disease detection.

Introduction

Viruses, among other infectious agents, often pose a serious threat to public health and the global economy because of the challenges in treating viral infections; therefore, early pathogen detection is important to ensure rapid diagnosis and treatment (1–3). Swift and reliable detection of viruses causing infectious diseases is crucial in a variety of medical fields, including ophthalmology, where infections caused by adenovirus (4), enterovirus

Competing Interest: H.T. is an employee of Aipore Inc. All other authors declare no competing interests.
Received: January 13, 2025. **Accepted:** May 1, 2025

(5), and cytomegalovirus (CMV) (6), pose a serious threat to vision. Indeed, the most common ocular viral insult is herpesvirus infection (7–9), which can lead to herpes keratitis (10), iridocyclitis, and acute retinal necrosis (11), all of which are potentially blinding conditions.

Herpesviruses are a group of double-stranded DNA viruses that can cause various diseases in humans and animals (12). There are eight known types of human herpesviruses (HHVs), classified into three subfamilies: alpha, beta, and gamma herpesviruses. Each type of herpesvirus has its unique characteristics and associated diseases (12, 13). Herpesvirus has a capsid containing the viral genome that is surrounded by a segment and envelope (12). The envelope of herpesviruses contains glycoproteins on its surface that facilitate binding and entry into host cells (12, 13). Herpesviruses are spherical particles of 100–200 nm diameter (Fig. 1a and b).

Currently, detecting an ocular viral infection prior to treatment is based on quantitative real-time (qRT) PCR of small samples of intraocular fluid (aqueous or vitreous humor), corneal swab, or tear film sample from the affected ocular surface (14). This method has excellent sensitivity; however, the assessment of the specific infectious pathogen itself is inaccurate because the method detects the nucleic acid genome. Additionally, the process from genome extraction to analysis is time-consuming and requires several hours, even in well-equipped medical institutions (15). To date, electrochemical sensors such as those based on nucleic acids, antibodies, and antigens have been used to detect viruses at the research level (16–18), although simultaneous detection of multiple viruses is difficult, and a clinically useful diagnostic method in terms of sensitivity and quantification has not been developed (19, 20). Furthermore, these sensors are difficult to transport and use and require expensive laboratory equipment; therefore, they are unsuitable for rapid clinical on-site analysis (21).

There are numerous approaches for detecting small molecules. One such modality, first developed to identify individual nucleotides in a DNA molecule (17, 21), is based on tunneling of small molecules through a solid-state nanopore in a thin silicon wafer, prompted by a tunneling current (19, 22). This approach was subsequently shown to be useful to identify individual bacterial cells (23), and more recently, influenza viruses in a physiological medium (24), and other viruses (20).

In the present study, we aimed to utilize the nanopore technology to identify and subclassify a range of herpesvirus particles in a label-free fashion and develop new tools based on machine learning and AI for simultaneous detection of multiple viruses. We also applied this approach to the clinical environment to show how viral (herpes) infection could be diagnosed in minutes in patients with suspected herpes infection.

Results

AI nanopore formation for viral discrimination

Each virus particle passing through the pore had a different size and surface charge, resulting in a corresponding change in impedance and a virus particle-specific waveform. An illustration of viral particles passing through the nanopore is shown in Fig. 1d. The virus particles move between the electrodes in the same manner as ion molecules, and the occlusion of the pores produces a change in the impedance, producing an ion waveform (Fig. 1e). The waveform is dependent on the size and surface charge of the virus particle and the unique molecular structure of the virus, including the virus surface glycoproteins (Fig. 1b). The morphologies of the viruses were characterized via ionic current spikes with wave heights (I_{ion}) and wave widths (t_d) (Fig. 1e). Virus-specific ionic current spikes derived from various parameters were extracted for the AI analysis.

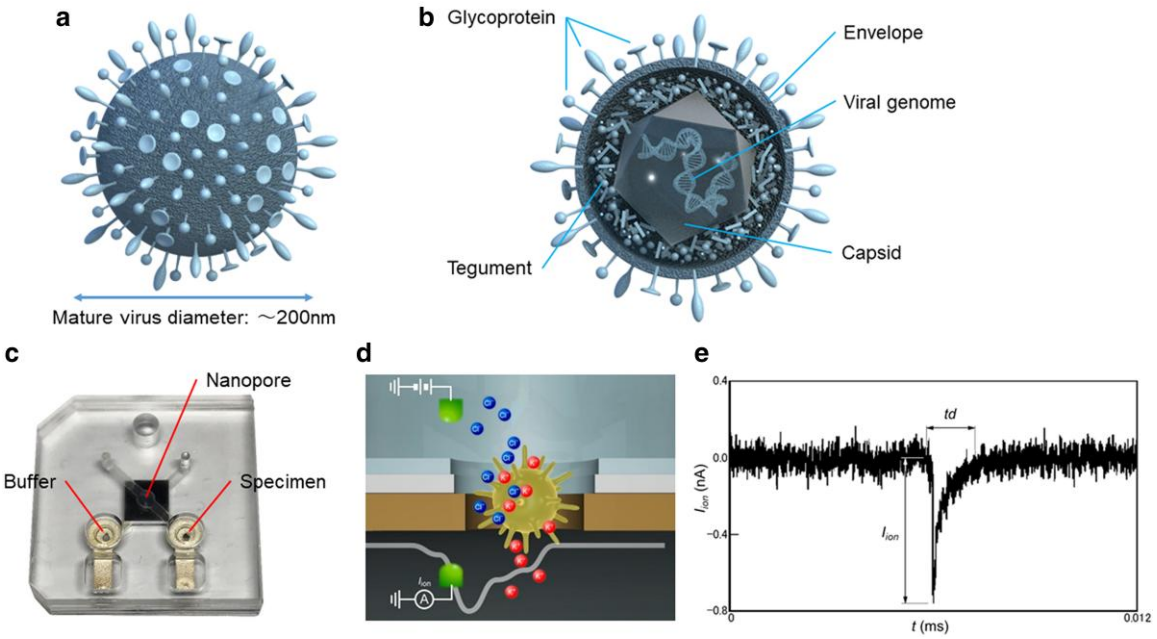

Fig. 1. Structure of the herpes virus, nanopore module, and its waveform. a) Schematic diagram of the herpesvirus. The mature herpesvirus diameter is ~200 nm. b) The virion consists of a capsid with an internalized viral genome covered by an envelope and protein spikes containing glycoprotein protruding from the surface. c) The module used for AI nanopore measurement. The voltage was applied across the nanopore (diameter: $d_{pore} = 300$ nm, thickness: $L_{pore} = 40$ nm) created in the SiN membrane. d) Schematic illustration of virus particles and ions passing through the nanopore and resistive pulse I_{ion} measurement. e) The ionic current I_p consists of spikes with height I_{ion} and width t_d corresponding to a single virus particle. Parameters I_{ion} and t_d show the amount of ion blockage and time of flight of the virus particles passing through the nanopore channel.

Detecting and discriminating cultured herpesviruses using AI

Information on the cultured viruses is provided in Table S1. When the cultured herpesviruses were measured at a voltage of −0.1 V, the ionic current–time waveform was observed as upward signals. One peak is equivalent to one viral particle. A number of measurement signals can be detected in just a few seconds. Live images of the waveforms of the cultured virus (herpes simplex virus [HSV]-1) are shown in Movie S1. Numerous waveforms were continuously detected. Representative waveforms for each virus are shown in Fig. 2a–f. The wave height corresponds to the current value (nA), and the wave width corresponds to the time (μs). The waveforms measured for the *Alphaherpesvirinae* subfamily (HSV-1 and varicella zoster virus [VZV]) (Fig. 2a and b) and *Betaherpesvirinae* subfamily (CMV, HHV6A, HHV6B, and HHV7) (Fig. 2c–f) were different. Moreover, different waveforms were observed within the same subfamily. The waveforms differed for each virus, with characteristic peaks that were further investigated using AI. The classifier learning accuracy of the two representative viruses was presented as a confusion matrix, which showed good discrimination via linear discrimination analysis. An *F*-value of >0.7 indicated that the results of this study were valid. An example of mapping to two dimensions using Fisher's linear discrimination analysis is shown in Fig. S1. The identification accuracy between CMV and HSV-1 showed a good discrimination score (*F*-measure [F_{mes}] = 0.836) (Fig. S1c and d). The identification accuracy between HSV-1 and VZV also showed a relatively good discrimination score (F_{mes} = 0.697) (Fig. S1a and b). The ionic current–time waveform was clearly different between HHV6A and HHV6B, the two subtypes of HHV6 (F_{mes} = 0.667) (Fig. S1e and f).

The discrimination analysis of combinations of various viruses indicated that three different types of viruses (HSV-1, VZV, and CMV) (Fig. S2) and four different types of viruses (HSV-1, VZV, CMV, and HHV7) can be identified with considerable accuracy (F_{mes} = 0.604 and F_{mes} = 0.775, respectively) (Figs. 2g and h and S3).

Detection and discrimination of viruses in clinical samples using the AI nanopore

Primary analysis of our cohort of patients with suspected viral infections showed that 60 of the 238 patients (25.2%) were positive for herpes infection based on qPCR analysis. Waveform data from the first 100 patients included 31 qPCR-positive cases (23 were positive for CMV, 3 were positive for VZV, 4 were positive for HSV-1, and 1 was positive for EBV) and 69 qPCR-negative cases. The waveform data from the remaining 138 patients comprised 29 qPCR-positive cases (20 positive for CMV, 5 positive for VZV, 2 positive for HSV-1, and 2 positive for HTLV-1), 76 qPCR-negative cases, and 33 healthy controls who underwent cataract surgery (Table S2). Based on the teacher data with correct answers from the qPCR test results, the first 100 waveforms were used as the dataset for training the AI, and the remaining 138 waveforms were used for the actual AI analysis. Clinical information and AI nanopore measurement results for each case are given in Table S3.

Representative waveforms for each virus from the clinical samples are shown in Fig. 3. AI nanopore devices can be installed in medical examination rooms in a space-efficient manner, enabling virus detection to be simultaneously performed with ophthalmological examination (Fig. 3a). In the aqueous humor of qPCR-positive cases, a waveform similar to that of the virus detected in the culture supernatant was observed (Fig. 3b–d). Each

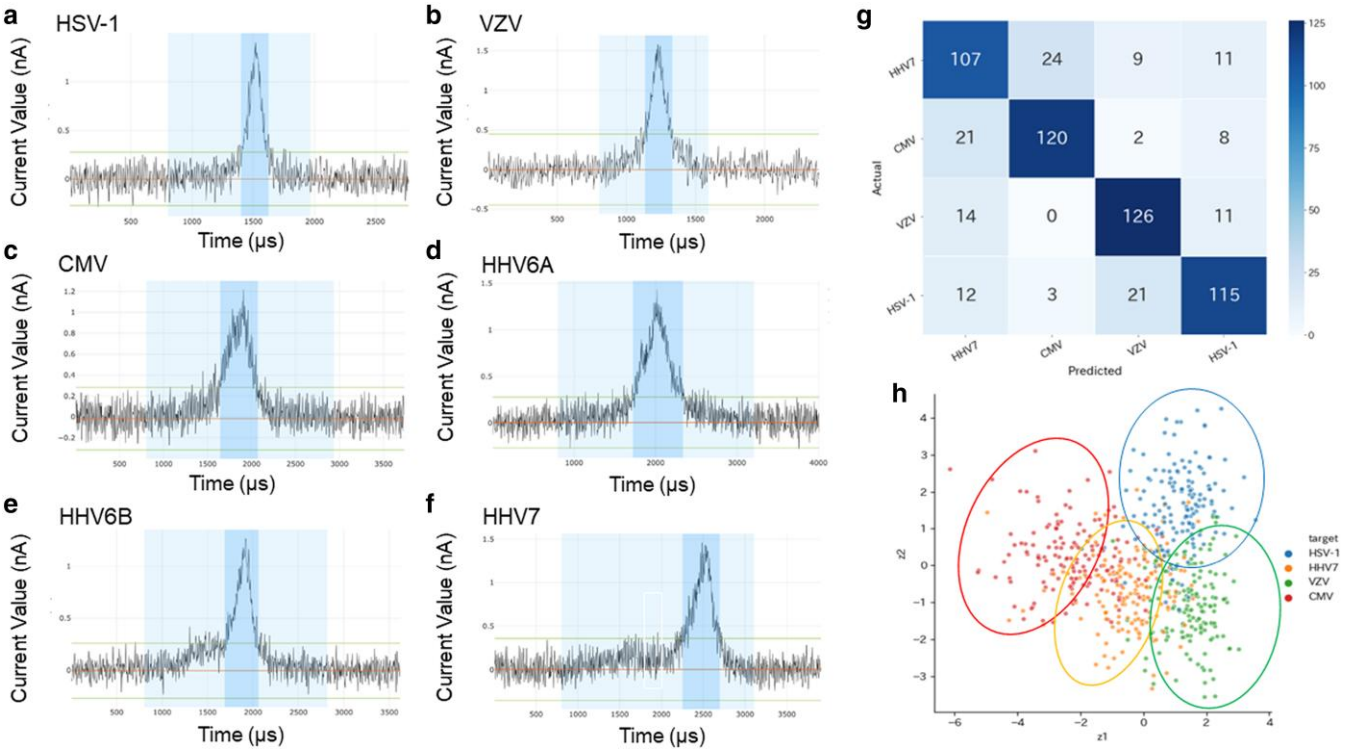

Fig. 2. Single herpes virus detection using the AI nanopore. Representative pulse waveforms for each of the cultured viruses were extracted from the waveforms obtained with the nanopore detector. a) HSV-1, b) VZV, c) CMV, d) HHV6A, e) HHV6B, and f) HHV7. g) In the confusion matrix based on the waveforms of all four viruses, each number in the matrix indicates the number of waveforms of the virus obtained from the nanopore measurements (F_{mes} = 0.775). h) Example of mapping to two dimensions using Fisher's linear discrimination analysis. The plot was mapped from a multivariate feature space to a 2D space of z_1/z_2, suggesting that the discriminative bounds of practical accuracy can be computed.

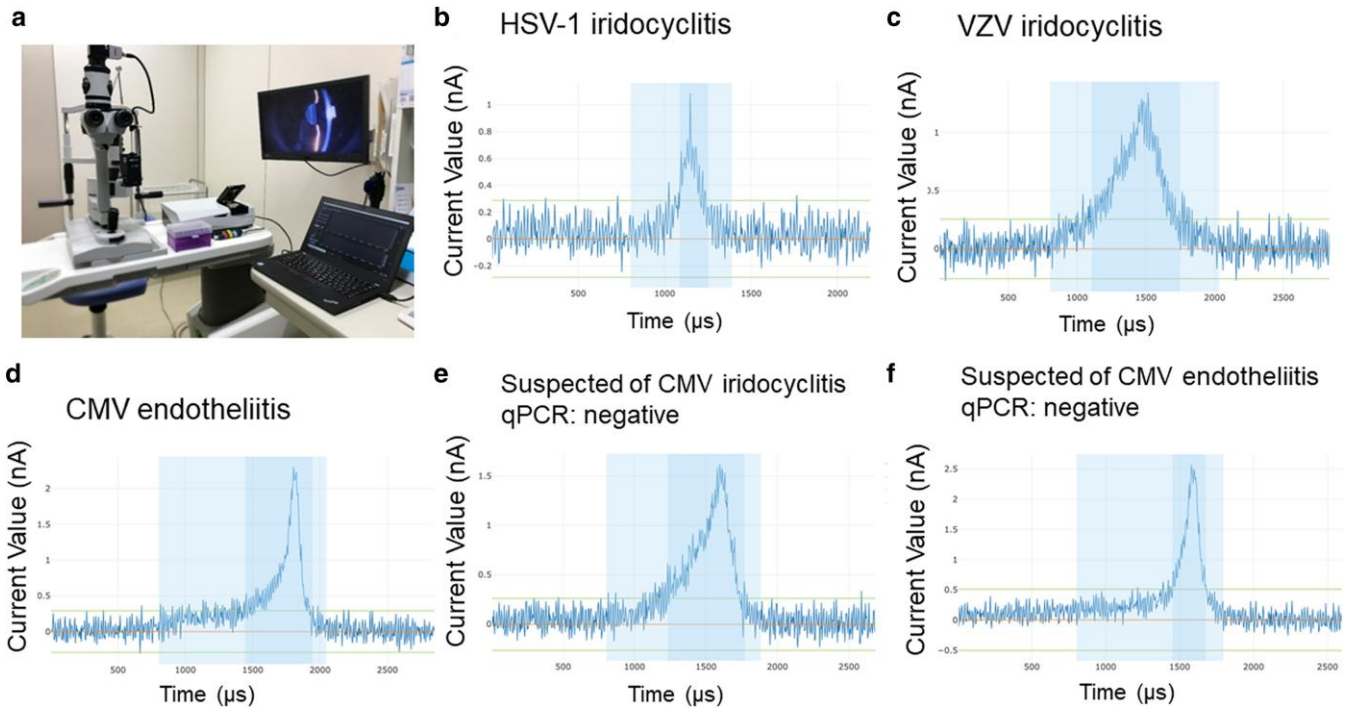

Fig. 3. Detecting viruses from clinical samples using the AI nanopore. a) The formation of an AI nanopore in an outpatient room is shown positioned right next to a slit-lamp microscope to enable immediate viral particle detection. Representative pulse waveforms for each clinical sample were extracted from the waveforms obtained by the nanopore detector. PCR-positive and PCR-negative groups are shown separately. The PCR-positive group comprised: b) a case of HSV-1 iridocyclitis (HSV-1: 2.3×10^5 copies/mL), c) a case of VZV iridocyclitis (VZV: 4.5×10^7 copies/mL), and d) a case of CMV endotheliitis (CMV: 1.5×10^5 copies/mL); the PCR-negative group included: e) a case of suspected CNV iridocyclitis and f) a case of suspected CNV endotheliitis.

of these cases was positive in the assessment using the AI nanopore, indicating the robustness of the detection procedure, which takes only a few minutes instead of several hours. Furthermore, a waveform characteristic of the virus was detected in a case of clinically suspected viral infection with negative qPCR result, suggesting the heightened sensitivity of the AI nanopore approach (Fig. 3e and f).

Discrimination of single CMV using the AI nanopore analysis

We subsequently analyzed the clinical cases of CMV infection using the AI nanopore. Based on the diagnostic criteria (25) and results of qPCR, 24 patients with clinically suspected CMV infection and 24 healthy controls were recruited for the analysis. Initially, we examined whether viral particles could be detected using PCR in patients who tested positive for CMV. Live images of clinical sample discrimination from patients with PCR-confirmed CMV endotheliitis are shown in Movie S2. The first waveforms began to appear 30–40 s after the start of the measurement, and within 1 min, we detected and identified CMV based on dozens of waveforms (Fig. 4 and Movie S2). Subsequently, we extracted many waveforms from CMV-positive patients and healthy controls for AI analysis and calculated the F_{mes} by identifying the waveforms using AI. In the analysis of 15 PCR-positive patients and 15 healthy controls, the pulse F_{mes} was 0.695 and assembled F_{mes}, which indicates case-by-case identification, was 0.792. The sensitivity and specificity were 100 and 71.4%, respectively. Subsequently, a comparison of 24 cases clinically diagnosed with CMV infection regardless of the PCR results and 24 healthy controls yielded an assembled F_{mes} of 0.75 and lower sensitivity of 45.8%, but a higher specificity of 91.7%.

Discussion

Timely detection of the infectious agent in cases of suspected viral infection can greatly aid in making an accurate diagnosis and providing appropriate patient treatment (26, 27). This is particularly important because disease progression may be rapid and clinicians are sometimes compelled to prescribe an antiviral medication as an insurance policy without any evidence of the true nature of the infection. In recent years, multiplex PCR systems have been commercialized, and they are capable of simultaneously detecting many pathogen types (14, 15, 18); however, the method is still time-consuming owing to the limited number of facilities available. In the present study, we successfully detected particles of the herpesvirus family members at the single-molecule level using a nanopore detector and discriminated among the viruses with high precision using an Al-based waveform analysis. This device can rapidly detect viral particles and can be useful as an on-site clinical diagnosis tool.

The AI nanopore can make a positive or negative decision for any clinical sample containing the target virus after learning the nanopore waveform of the virus being measured (23). In the present study, we used the aqueous humor as the source; however, any tissue can be used as the source as it can be readily homogenized, and virus particles can be detected without pretreatment, such as the extraction of nucleic acids or proteins, making it possible to rapidly detect them (Fig. 5). Detecting viral particles using enzyme-linked immunosorbent assay can be challenging without preestablished specific antibodies. Although the multiplex PCR method can detect different viruses, it can only detect the viruses for which the primer is set. Additionally, PCR detects the presence of viral particles via genome detection and has the disadvantage of detecting viral particles regardless of their viability (17, 18). AI nanopore solves these problems and enables single-molecule

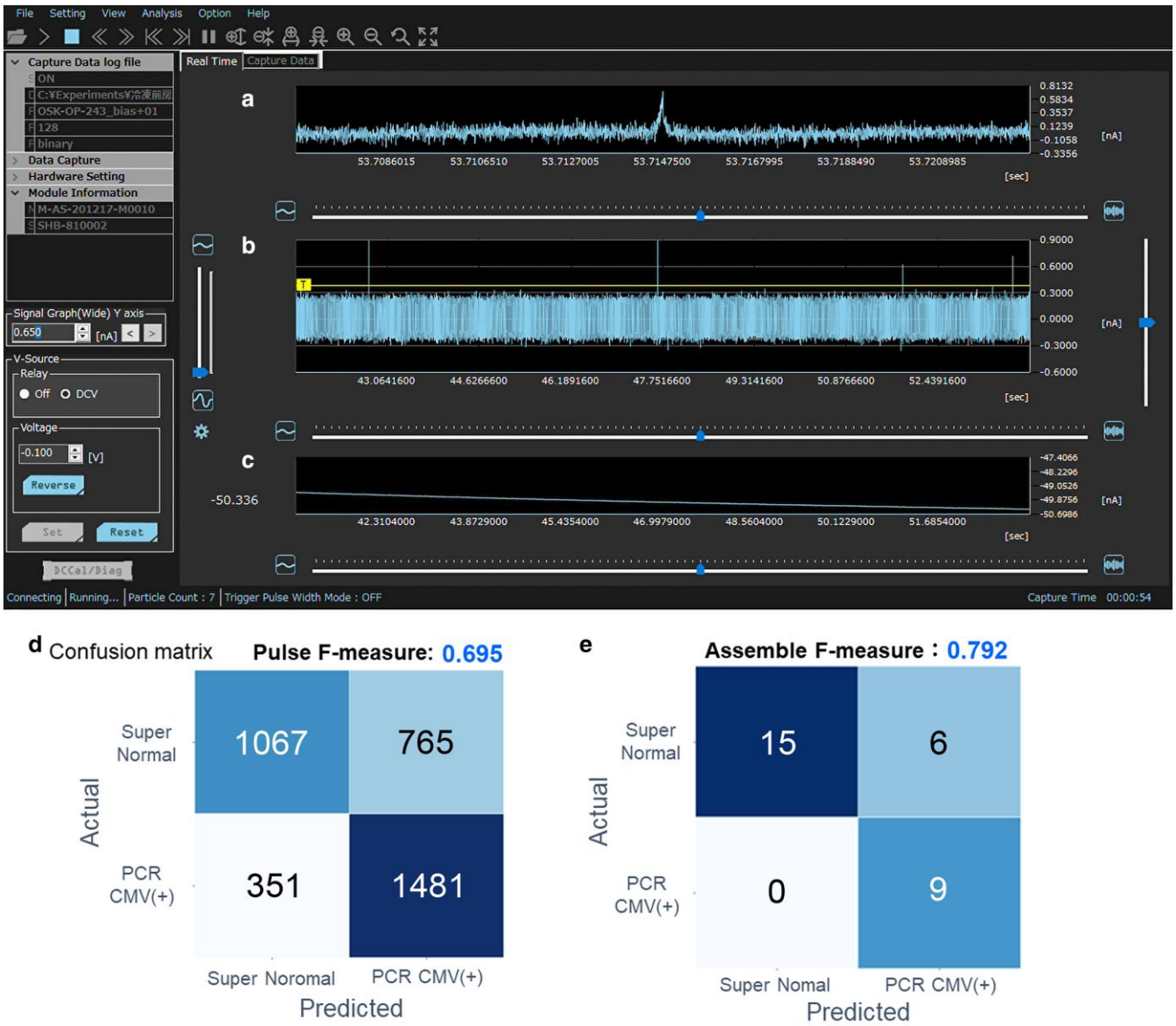

Fig. 4. Measuring and discriminating clinical samples using the AI nanopore. The measurement screen after loading the clinical sample (CMV: 1.8×10^5 copy/μL) into the nanopore is shown. The waveform was observed 30 s after the start of the measurement, and virus particles were successively detected. a) The upper window shows the waveform corresponding to a single p r detected by the nanopore detector. b) The middle window shows the continuously observed wide baseline and occasionally a spike signal corresponding to a single virus particle. c) The lower window shows changes in the current flowing through the nanopore detector. Each number in the matrix indicates the number of virus waveforms obtained by the AI nanopore measurement, as shown in d) and e). The F_{mes} was calculated based on these confusion matrices. a) Pulse F_{mes}: CMV-positive patients vs. normal controls ($F_{mes} = 0.695$); b) assemble F_{mes}: CMV-positive patients vs. normal controls ($F_{mes} = 0.792$).

detection of live viral particles. A certain virus concentration is necessary because a specific number of virus particles must be present in the vicinity of the nanopores; however, as one waveform corresponds to one copy, there is no detection threshold, which is a limitation of the conventional PCR method (28). Conversely, high concentrations of viral particles pose a measurement challenge. Although the initial few waveforms can be detected, the sheer number of particles around the pore interferes with accurate assessment due to occlusion. To circumvent this issue, all viral solutions were diluted to 10^4 copies/mL, ensuring that any sample, irrespective of its density, could be measured. Furthermore, if a pass-through waveform is obtained, the presence of some particles in the sample can be estimated, even if a waveform other than that of a learned virus is tentatively detected.

AI nanopore analysis using cultured viruses revealed that *Alphaherpesvirinae* and *Betaherpesvirinae* species can be distinguished with relatively high accuracy within the same *Herpesviridae* family. A high discrimination accuracy was achieved between two virus types and among three and four virus types, suggesting that simultaneous detection of virus particles is possible even when multiple viruses coexist in a sample. HHV6A and HHV6B subtypes could be accurately distinguished using the AI nanopore despite having over 90% genome sequence homology (29). Thus, the AI nanopore technology can rapidly identify viruses without genome sequencing.

In the AI nanopore analysis using clinical samples, we primarily focused on CMV owing to the high number of CMV-positive patients in our case series. Human cytomegalovirus (HCMV), a

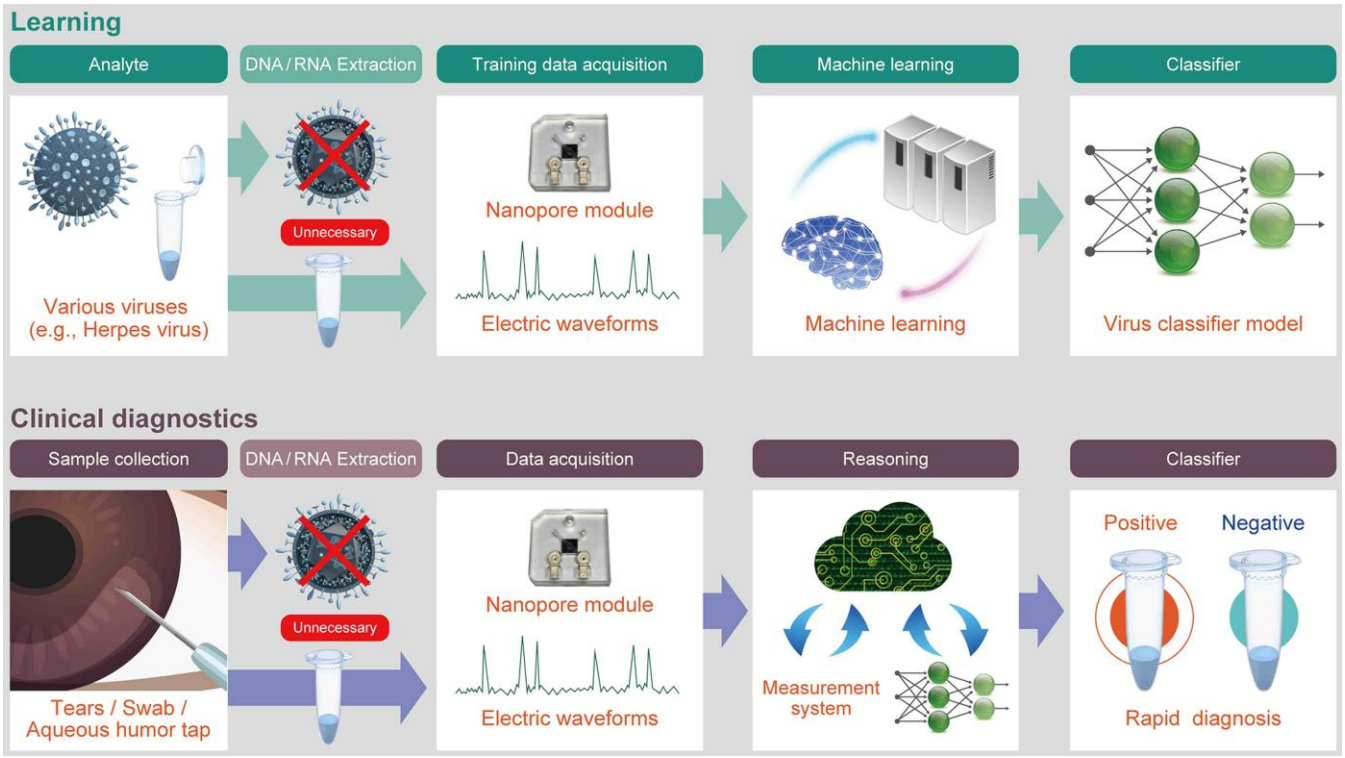

Fig. 5. Implementation of the AI nanopore for rapid viral particle detection. The novel scheme utilizing AI nanopore for rapid viral particle detection. This process involves two distinct phases: learning and clinical diagnosis phases. During the learning phase, training data were collected from specimens that were known to contain viral particles. Machine learning algorithms were then applied to the data to train the AI model. During the clinical diagnosis phase, clinical specimens were directly analyzed using nanopores, eliminating the need for DNA/RNA extraction. Subsequently, the obtained waveforms were analyzed using the pretrained AI model, enabling swift and accurate virus identification. This approach offers a promising solution for expediting viral detection without cumbersome sample preparation procedures.

member of the *Betaherpesvirinae* subfamily of the family *Herpesviridae*, is a common cause of herpesvirus infection in immunocompetent individuals and immunocompromised hosts (6, 29). The virus structure consists of three virion proteins: the nucleocapsid, tegument, and envelop, and the virion is ~220 nm in diameter (12). HCMV infections have been linked to various serious systemic infectious diseases including pneumonia, coronary heart disease, inflammatory bowel disease, and eye diseases (6, 12, 25). Early and sensitive detection of HCMV is important to ensure good patient prognosis and is crucial in the field of ophthalmology from the viewpoint of visual outcome. The AI nanopore accurately identified clinical samples with high discrimination. The discrimination accuracy between the PCR-positive CMV group and negative controls had 100% sensitivity. The waveform was even detected in cases where CMV infection was clinically suspected, but the samples were PCR-negative, demonstrating high sensitivity of the AI nanopore. We compared all clinical diagnosis groups with a negative control group of cases with negative PCR results but clinically suspected CMV infection, together with the PCR-positive group. Although the sensitivity was low because PCR positivity was used as the correct data, the specificity was 91.7% or higher, indicating that the diagnosis by AI nanopore is closer to the actual judgment of the clinician.

Virome analysis was additionally performed on the variation of sensitivity and specificity with condition. Analysis of the normal control group revealed that viral genomes were also detected in samples that tested negative for PCR (Supplementary Table S4). Unsurprisingly, the presence of viral genomes was more prevalent in PCR-positive samples. Consequently, we determined that the samples that tested negative for PCR and were utilized as normal controls could not be authentic negative controls. The qPCR method has a detection limit of ~10^3 copies/mL. Additionally, the nanopore measurements that can detect a single viral particle molecule are too sensitive for detection and are therefore judged to be false positives. Therefore, cases with a viral concentration of 10^2 copies/mL or less and a negative qPCR result are classified as positive for nanopore measurement. For these reasons, if the PCR results are taken as correct, a decrease in sensitivity cannot be avoided.

The initial approach involves the utilization of sequencing analysis as an alternative to PCR for the labeling process, particularly when the subject is considered healthy. This enhancement can be achieved through two methods: first by extending the measurement time and second by implementing a preliminary treatment to concentrate the specimen prior to measurement. Moreover, while machine learning was employed in this study, an alternative approach involves the augmentation of the number of pulses and specimens, which could be facilitated by the implementation of deep learning methodologies. This study was limited by the small sample, which is a consequence of the low incidence of herpesvirus infection. Furthermore, only *Herpesviridae* species were used in the analysis. A more comprehensive search of methods for quantifying and detecting pathogenic viruses in tissues other than the eye is needed.

In the present study, we showed that rapid on-site diagnosis of ocular viral infection can be achieved using solid-state nanopore analysis combined with AI. As technology develops and costs come down, this technique represents an excellent alternative

to qRT-PCR in the clinician armory to combat viral ocular infections, with important implications for other branches of medicine (Fig. S4). This device can detect viral particles in a very short time without pretreatment and can be a valuable on-site diagnostic modality.

Materials and methods

Electrical measurements with a nanopore device

A nanopore measurement device (NanoSCOUTER; Advantest, Tokyo, Japan) and nanopore module (Aipore Co., Ltd., Tokyo, Japan) were used as previously described (30). A solid-state nanopore with a diameter (d_{pore}) of 300 nm was sculpted in a SiN membrane with a thickness (L_{pore}) of 40 nm on an Si wafer with an aspect ratio of 0.01. The module used for AI nanopore measurements is shown in Fig. 1c. The Ag/AgCl electrodes were placed on both sides of the nanopore. The principle of measurement using the nanopore module is shown in Movie S3. Briefly, 15 μL of the buffer solution (BSS plus irrigation solution; Alcon Laboratories, Inc., Fort Worth, TX, USA), with a chemical composition similar to that of aqueous and vitreous humor, was injected into each side of the nanopore module and the cross-membrane ionic current (I_{ion}) was measured after applying a base current dc voltage (V_b) of 0.1 V. After confirming nanopore formation, one side of the nanopore module was replaced with 15 μL of virus sample suspended in the buffer solution. As the viral particles pass through the pore, they occlude the pore according to their size and surface charge and change the impedance, resulting in a waveform pattern specific to the virus. The principles and procedures for virus detection using the nanopore detector are shown in Movie S4. We obtained various viral particles from the supernatants of infected cell cultures and clinical samples.

AI-based analytical methods

The virus type was identified using AI nanopore analysis of the characteristic patterns of the viruses. The development of the AI nanopore platform has been previously described (30). The ionic current–time waveform obtained with nanopore measurement was analyzed using the following procedure with the machine learning system Aipore-ONE provided by Aipore Inc. (Tokyo, Japan). The AI estimates the baseline waveform and measures the time from the appearance of the waveform and crossing the baseline until it returns to the baseline, and the time from the baseline to the appearance of the waveform peak. The virus ionic current–time waveforms were obtained, automatically extracted, and classified using the learning model. Several machine learning algorithms—random forest (RF) and support vector machine, a data-driven analytic approach that specializes in the integration of a wide range of datasets into patterns that can be used for prediction—were used. RF was used as the machine learning algorithm. Classifier learning was performed using features such as the wave height (I_{ion}) and wave width (t_d). The classification accuracy of the viruses was evaluated using F_{mes}. The definition of F_{mes} is shown in Fig. S5. Using F_{mes} as an index, a classifier that produced the highest F_{mes} was selected. $F_{mes} = 1$ corresponds to 100% accuracy. The data and classifier that produced the highest F_{mes} were designated as the teacher data and learning model, respectively. The machine learning model and calculation of the reliability of identification using annotated waveforms are shown in Fig. S6. Comparison and consistency of the waveforms with different batches of the same viruses are shown in Fig. S7.

Preparing cultured viruses

A series of known herpesvirus particles was purchased from the American Type Culture Collection (Manassas, VA, USA) Virology Collection. The viruses included human herpesvirus 1 (HSV-1), human herpesvirus 3 (VZV), and HHV6B (strain: HST, VR-1467). HSV-1 (KOS strain), VZV (pOka strain), HCMV (VR-1590 strain), HHV6A (GS strain), and HHV7 (KHR strain) were provided by Professor Yasuko Mori. For the preparation of cultured viruses, Vero, MRC-5, MT4, HSB-2, and SupT1 cells were seeded in complete α-modification of minimal essential media (Corning CellGro, Corning, NY, USA) or Rose Park Memorial Institute medium with 10% fetal bovine serum (Thermo Fisher Scientific, Waltham, MA, USA) and grown at 37 °C under 5% CO_2 in a humidified atmosphere. HSV-1, VZV, HHV6B, HHV6A, and HHV7 cells were propagated in Vero, MRC-5, MT4, HSB-2, and SuT1 cells, respectively. The viruses were propagated in cultured cells until maximal cytopathic effects were reached. The cells were lysed by freezing and thawing once. Cell debris was removed via centrifugation at 1500 *g* for 5 min at 4 °C. The supernatants were used for viral detection. Information on the cultured viruses is provided in Table S1. To circumvent the occurrence of pore occlusion as a consequence of elevated concentrations of virus solution, a dilution process was employed, reducing the concentrations of all samples to 10^4 copies/mL prior to measurement. Experiments with all viruses were conducted after obtaining approval of the Gene Modification Experiment Safety Committee of Osaka University (approval number: 04320) and were performed at the BSL-2 level of experimentation.

Clinical sample collection from patients

Recruitment began on 2019 March 1 when the AI nanopore detection equipment setup was completed and a system capable of stable measurement under certain conditions was established, and ended on 2021 December 31 when the sample size used for opportunity learning and that for the actual measurement was almost the same. During this period, 205 consecutive patients who visited the patient portal at Osaka University Hospital, Japan, were diagnosed with a suspected ocular viral infection and underwent aqueous humor sampling. In this observational case series, we examined the aqueous humor of patients with herpetic iridocyclitis, endotheliitis, and retinitis. Aqueous humor samples of 33 healthy individuals with no history of systemic and/or ocular infection were obtained at the time of cataract surgery and served as healthy controls. The sample size was not measured because it was unknown what kind of data would be obtained from the AI nanopore measurement and the parameter settings could not be predicted. Medical records were retrospectively reviewed. A diagnosis of herpesvirus infection was made based on clinical symptoms, such as corneal (keratitis, stromal keratitis, endotheliitis, keratic precipitates, and increased intraocular pressure) and retinal or vitreous lesions (retinal vasculitis, vitreous cells). The final diagnosis of viral infection was confirmed by detecting antigenemia or the viral genome using conventional PCR. Viral DNA copy numbers were calculated by the Research Institute for Microbial Disease, Osaka University, according to previous reports (14, 15). The demographic data of the patients and causative virus information are given in Table S3. All patients provided written informed consent for the investigation, and the study adhered to the tenets of the Declaration of Helsinki. This study was approved by the local ethics committee of Osaka University Medical Hospital (approval ID: 202253). This clinical study was

registered at the University Hospital Medical Information Network (UMIN) under UMIN000043968.

Analyzing discrimination between viruses and usefulness of the AI nanopore for clinical diagnosis

The nanopore detector setup was completed in a safety cabinet for the analysis of cultured viruses, and the waveforms were obtained by directly measuring the supernatants of the virus-infected cell cultures with the AI nanopore. The waveforms obtained during the 10-min measurement were analyzed using AI for virus discrimination. For the analysis of clinical samples, the nanopore detector was set up in advance in an outpatient setting, and virus detection was immediately performed (within minutes) without cryopreservation after collecting the anterior chamber fluid. Viral waveforms obtained during the 10-min sample detection time were analyzed as the waveform data. Based on teacher data with correct answers from the multiplex qPCR test results, the waveform data from the first 100 patients and healthy controls were used as the dataset for training the AI. Waveform data from the remaining 105 patients were used for the actual analysis. The diagnostic accuracy of the AI nanopore detector for viruses was analyzed using F_{mes}.

Supplementary Material

Supplementary material is available at *PNAS Nexus* online.

Funding

This research was supported by the Japan Society for the Promotion of Science (JSPS) KAKENHI (grant numbers 21K09695 and 24K12804) and International Joint Research Promotion Program of Osaka University. This work was also supported by the Integrated Frontier Research for Medical Science Division, Institute for Open and Transdisciplinary Research Initiatives, Osaka University.

Author Contributions

N.H., Y.M., and K.N. designed the study. N.H., T.S., Y.O., K.M., and L.H. collected the data. N.H., H.T., M.T., N.N., and A.Q. analyzed the data and vouch for the data and the analyses. All authors contributed to the writing of the paper, reviewed the manuscript, and amended or approved the final version. N.H. was responsible for the decision to submit the manuscript for publication.

Data Availability

All data are included in the manuscript and/or supporting information.

References

1 Baker RE, *et al.* 2022. Infectious disease in an era of global change. *Nat Rev Microbiol.* 20:193–205.
2 Moeti M, Gao GF, Herrman H. 2022. Global pandemic perspectives: public health, mental health, and lessons for the future. *Lancet*. 400:e3–e7.
3 Vallée A. 2023. Geoepidemiological perspective on COVID-19 pandemic review, an insight into the global impact. *Front Public Health.* 11:1242891.
4 Lynch JP 3rd, Kajon AE. 2016. Adenovirus: epidemiology, global spread of novel serotypes, and advances in treatment and prevention. *Semin Respir Crit Care Med.* 37:586–602.
5 Pons-Salort M, Parker EPK, Grassly NC. 2015. The epidemiology of non-polio enteroviruses: recent advances and outstanding questions. *Curr Opin Infect Dis.* 28:479–487.
6 Joye A, Gonzales JA. 2018. Ocular manifestations of cytomegalovirus in immunocompetent hosts. *Curr Opin Ophthalmol.* 29: 535–542.
7 Sudesh S, Laibson PR. 1999. The impact of the herpetic eye disease studies on the management of herpes simplex virus ocular infections. *Curr Opin Ophthalmol.* 10:230–233.
8 Feng Y, *et al.* 2024. Viral anterior uveitis: a practical and comprehensive review of diagnosis and treatment. *Ocul Immunol Inflamm.* 32:1804–1818.
9 Radosavljevic A, Agarwal M, Chee SP, Zierhut M. 2022. Epidemiology of viral induced anterior uveitis. *Ocul Immunol Inflamm.* 30:297–309.
10 Rowe AM, *et al.* 2013. Herpes keratitis. *Prog Retin Eye Res.* 32: 88–101.
11 Servillo A, *et al.* 2023. Posterior herpetic uveitis: a comprehensive review. *Ocul Immunol Inflamm.* 31:1461–1472.
12 Liu F, *et al.* 2007. Comparative virion structures of human herpesviruses. Chapter 3. In: *Human herpesviruses: biology, therapy, and immunoprophylaxis*. Cambridge: Cambridge University Press.
13 Kornfeind EM, Visalli RJ. 2018. Human herpesvirus portal proteins: structure, function, and antiviral prospects. *Rev Med Virol.* 28:e1972.
14 Sugita S, *et al.* 2013. Use of a comprehensive polymerase chain reaction system for diagnosis of ocular infectious diseases. *Ophthalmology*. 120:1761–1768.
15 Sugita S, Takase H, Nakano S. 2023. Role of recent PCR tests for infectious ocular diseases: from laboratory-based studies to the clinic. *Int J Mol Sci.* 24:8146.
16 Dhama K, *et al.* 2019. Biomarkers in stress related diseases/disorders: diagnostic, prognostic, and therapeutic values. *Front Mol Biosci.* 6:91.
17 Yuwen L, Zhang S, Chao J. 2023. Recent advances in DNA nanotechnology-enabled biosensors for virus detection. *Biosensors (Basel)*. 13:822.
18 Nguyen TN, Phung VD, Tran VV. 2023. Recent advances in conjugated polymer-based biosensors for virus detection. *Biosensors (Basel)*. 13:586.
19 Tsutsui M, Taniguchi M, Kawai T. 2009. Transverse field effects on DNA-sized particle dynamics. *Nano Lett.* 9:1659–1662.
20 Darvish A, *et al.* 2019. Mechanical characterization of HIV-1 with a solid-state nanopore sensor. *Electrophoresis*. 40:776–783.
21 Xiao M, *et al.* 2022. Virus detection: from state-of-the-art laboratories to smartphone-based point-of-care testing. *Adv. Sci. (Weinh)*. 9:e2105904.
22 Dekker C. 2007. Solid-state nanopores. *Nat Nanotechnol.* 2: 209–215.
23 Tsutsui M, *et al.* 2017. Discriminating single-bacterial shape using low-aspect-ratio pores. *Sci Rep.* 7:17371.
24 Arima A, *et al.* 2018. Selective detections of single-viruses using solid-state nanopores. *Sci Rep.* 8:16305.
25 Koizumi N, *et al.* 2015. Clinical features and management of cytomegalovirus corneal endotheliitis: analysis of 106 cases from the Japan corneal endotheliitis study. *Br J Ophthalmol.* 99:54–58.
26 Meckawy R, Stuckler D, Mehta A, Al-Ahdal T, Doebbeling BN. 2022. Effectiveness of early warning systems in the detection of infectious diseases outbreaks: a systematic review. *BMC Public Health*. 22:2216.

27 Gradisteanu Pircalabioru G, *et al.* 2022. Advances in the rapid diagnostic of viral respiratory tract infections. *Front Cell Infect Microbiol*. 12:807253.
28 Yuan JS, Reed A, Chen F, Stewart CN Jr. 2006. Statistical analysis of real-time PCR data. *BMC Bioinform*. 7:85.
29 Ablashi D, *et al.* 2014. Classification of HHV-6A and HHV-6B as distinct viruses. *Arch Virol*. 159:863–870.
30 Taniguchi M, *et al.* 2021. Combining machine learning and nanopore construction creates an artificial intelligence nanopore for coronavirus detection. *Nat Commun*. 12:3726.